Agricultural and Forest Meteorology 264 (2019) 334–342

Contents lists available at ScienceDirect

Agricultural and Forest Meteorology

journal homepage: www.elsevier.com/locate/agrformet

Analysis of the spatiotemporal variability of droughts and the effects of drought on potato production in northern China

Yandong Wang[a,b], Xiaoli Liu[a,c], Guangxin Ren[a,b], Gaihe Yang[a,b], Yongzhong Feng[a,b,*]

[a] College of Agronomy, Northwest A&F University, Yangling, 712100, Shaanxi, China
[b] Shaanxi Engineering Research Center of Circular Agriculture, Yangling, 712100, Shaanxi, China
[c] Institute of Water Saving Agriculture in Arid Areas of China, Northwest A&F University, Yangling, 712100, Shaanxi, China

ARTICLE INFO

Keywords:
Potato
Drought variability
Standardize precipitation evapotranspiration index
Margins of the Asian monsoon
Agro-pastoral ecotone

ABSTRACT

Knowledge about drought variability in the main potato producing areas can provide a scientific basis for management of potato crops. In this study, the variations and patterns of drought in the potato growing period (GP), seedling stage (SS), tuber-growth stage (TS), and mature stage (MS) identified by the Standardized Precipitation Evapotranspiration Index (SPEI) were investigated in the north single cropping zone (NSCZ) in China for the period of 1960–2016 based on the empirical orthogonal function analysis, Mann–Kendall statistical test, Mann–Kendall test, Sen's slope, Hurst exponent, and continuous wavelet transform. Additionally, grey theory was used to study the relationship between drought and potato production. The results of the study follow: 1) The spatiotemporal patterns of drought of the two leading patterns were identified. 2) Since the 1970s, the NSCZ has become drier in the GP and MS, has become wetter in the TS, but has always remained in an unstable state of alternating wet and dry conditions in the SS. 3) The changes in dryness/wetness conditions include significant periodic oscillation features. 4) The future drought trend is generally consistent with the current state. In addition, it is worth noting that the NSCZ as a whole will become drier in the MS. 5) The drought of SS and TS had a relatively large negative effect on potato production, whereas that of MS had a relatively small positive effect. Because the NSCZ is within the marginal region of the Asian monsoon and the agro-pastoral ecotone, it is an ecologically fragile region. Therefore, under the background of global climate change, studying changes in dryness/wetness conditions has important implications for the ecological security and potato production of the region.

1. Introduction

Over the past 100 years, extreme weather events such as storms, heat waves, floods, and droughts have been abruptly and acutely felt due to climate change (Tong et al., 2018; Walther et al., 2002). Among these, drought is an extreme meteorological event characterized by below normal rainfall over a period of months to years (Dai, 2011). Drought substantially impacts agricultural production, water resources, and ecosystems, and it can cause economic losses, famine, epidemics, and land desertification (Beguería et al., 2010; Liu et al., 2013; Lobell and Field, 2007; Tao et al., 2006; Yuan et al., 2010).

Potato (*Solanum tuberosum* L.) is one of the most important crops in the world (Tian et al., 2003). China has been the world's largest potato producer since 1993, and potato is the fourth largest food crop after rice, wheat, and corn (Wang et al., 2018). The north single cropping zone (NSCZ), where most (approximately 85%) of the potato production occurs, includes the northeast, North China, and northwest potato-dominant areas (Jansky et al., 2009) (Fig. 1a). As a result of the regionally cool climate, abundant sunshine, and large daily temperature differences in the NSCZ, potato is a suitable crop for producing fresh food, as well as for starch processing and seed potato. While the total yield and yield per unit area of potato in the NSCZ have exhibited long-term increases, they have also shown large interannual fluctuations (Figs. A.3 and A.4). Therefore, potato production is not only affected by technical progress, such as breeding and field management practices, but also by climate factors.

Potato is the main crop in the NSCZ (Hu et al., 2014). However, the NSCZ borders the Tibetan Plateau, Loess Plateau, and Mongolian Plateau. It is within the marginal region of the Asian monsoon and is influenced by both the Asian monsoon and the westerlies (Li et al., 2012)

Abbreviations: EOF, empirical orthogonal function; CWT, continuous wavelet transform; H, Hurst; GP, growing period; SS, seedling stage; TS, tuber-growth stage; MS, mature stage; SPEI, standardized precipitation evapotranspiration index; NSCZ, north single cropping zone

* Corresponding author at: College of Agronomy, Northwest A&F University, Yangling, 712100, Shaanxi, China.
E-mail address: fengyz@nwsuaf.edu.cn (Y. Feng).

https://doi.org/10.1016/j.agrformet.2018.10.019
Received 4 June 2018; Received in revised form 14 October 2018; Accepted 26 October 2018
Available online 07 November 2018
0168-1923/ © 2018 Elsevier B.V. All rights reserved.

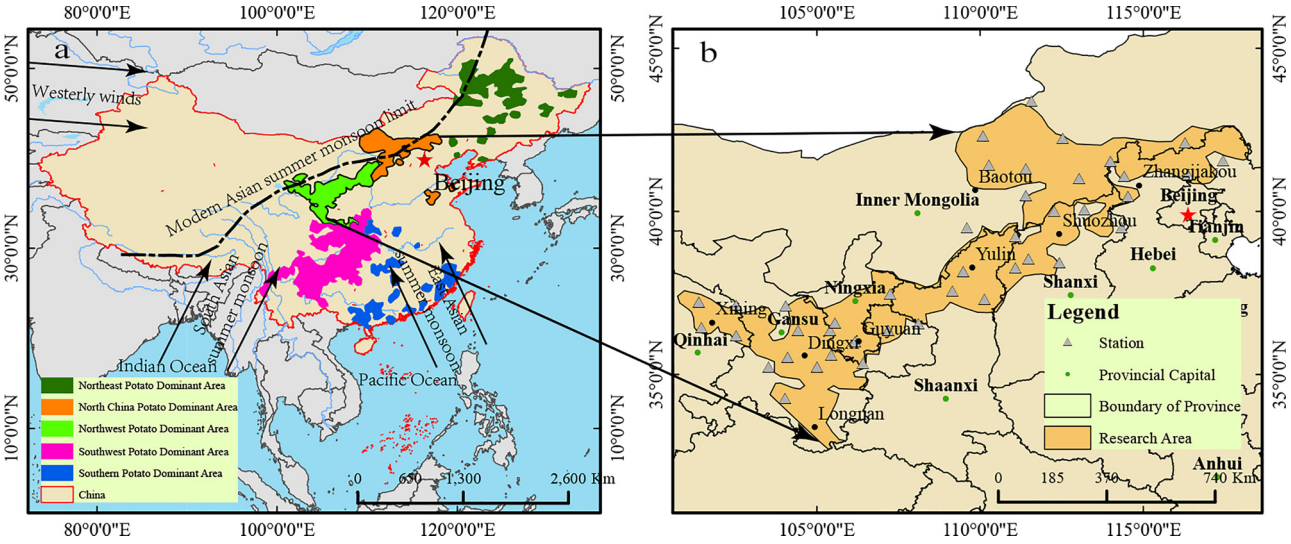

Fig. 1. Map of climate systems (Li et al., 2012) (a) and potato dominant area (Policy Plan, 2009) (b).

(Fig. 1a). As a result of its landlocked location coupled with the role of the plateau topography, a climatic background of drought has developed within the NSCZ. Moreover, the thermal and dynamic effects of the plateau topography, together with the interannual changes in the prevailing circulation, have caused changes in interannual dryness/wetness conditions (Song, 2005). The NSCZ is within the agro-pastoral ecotone of northern China, an ecologically fragile region that is highly sensitive to climate change (Zhao et al., 2017). It is also part of a rain-fed agricultural region that lacks water resources and has poor irrigation capacity, so crops are vulnerable to drought. Tian et al. (2003) and Zhao et al. (2014) showed that drought is the key limiting factor for potato production in the NSCZ.

With the aggravation of global climate change, it has been predicted that the overall simulated global potato yields will decrease by between 10% and 19% in 2010–39, and 18% and 32% in the 2050s if no adaptation is considered (Hijmans, 2003). Potato is often considered as a drought sensitive crop, and its sustainable production is threatened by frequent episodes of drought (Obidiegwu et al., 2015). Potato roots relatively shallowly (its roots are assumed to grow to a depth of about 60 cm), and water availability depends on precipitation (infiltration), percolation, soil surface evaporation, and crop transpiration (Haverkort and Verhagen, 2008). Drought not only reduces potato yield, considering that the crop may extract less available water from the soil in comparison with other crops, but can also harm product quality, for example, by increasing the incidence of common scab (Obidiegwu et al., 2015). Monneveux et al. (2013) showed that "drought decreases plant growth, shortens the growth cycle, and reduces the number and size of tubers and that short periods of drought during tuber bulking lead to dumbbell-shaped, knobby, or pointed-end tubers. Water limitation reduces leaf growth, leaf area index, ground coverage, rate of photosynthesis per unit of leaf area ($\mu CO_2\,m^{-2}\,s^{-1}$), and harvest index". In 2010, drought caused a 30% loss of processing potato production in central Russia and the Volga Valley region of Russia, and potato yields in Poland were reduced by ~30% because of water deficit (Obidiegwu et al., 2015).

Drought is classified into three types: meteorological drought, agricultural drought, and hydrological drought (Dai, 2011); however, meteorological drought is a prerequisite for the other types (Tong et al., 2018). Many studies have developed drought indices to quantify and analyze droughts (Dai, 2011; Liu et al., 2018; Yao et al., 2018). These drought indices may be divided into standardized, non-standardized, and comprehensive indices. Non-standardized drought indices are usually obtained from numerical calculations using several simplistic variables, but their ranges for classifying drought levels differ. The calculations for standardized drought indices are relatively complex, but these indices have uniform classification criteria and are comparable. The comprehensive drought index combines the aforementioned indices. The advantages of standardized drought indices make them the most widely used of these three approaches. Standardized drought indices include the Palmer Drought Deverity Index (PDSI), Standardized Srecipitation Index (SPI), and Standardized Precipitation Evapotranspiration Index (SPEI). The PDSI lacks multiscale drought characteristics, and while the SPI can be used for multiscale comparisons, it only includes precipitation, not the drought conditions caused by climate warming. The SPEI is an improvement of the SPI that includes temperature in the calculation so that the resulting drought includes the effects of climate warming (Yao et al., 2018). Therefore, the SPEI has certain advantages for the study of drought, and it has been used widely for this purpose.

Drought has an important impact on potato production. Although there is a great deal of research on methods to relieve the effects of drought on potato production, such as breeding of drought-tolerant varieties based on genetics (Banik et al., 2016; Evers et al., 2010), water-saving irrigation (Yactayo et al., 2013), cropping systems (Hu et al., 2014), etc., there continues to be a paucity of spatiotemporal analyses and predictive research of drought in potato production areas. The NSCZ is a large ecologically fragile area, and the mode of agricultural production, which relies on rainfall, has not changed much over time. Therefore, this study utilizes the SPEI drought index to study (1) the relationship between potato production and drought, (2) the spatiotemporal characteristics of drought, and (3) drought trends in the future forecast from the periodic features and long-term drought trends in the NSCZ. This study aims to provide a theoretical basis for studying drought in the marginal Asian monsoon region in the context of global climate change and for potato field management and breeding in rain-fed agricultural and ecologically fragile areas.

2. Material and methods

2.1. Study area and dataset

In order to ensure the continuity of the study area, the NSCZ did not include the northeast potato-dominant area and parts of Shandong Province, and only covers some parts of Gansu, Ningxia, Shaanxi, Inner Mongolia, Shanxi, Hebei, and Qinghai Provinces (Fig. 1b). The mean annual rainfall in this area is 250–500 mm, 60–70% of which occurs from June-August (Lu and Jia, 2013; Tian et al., 2003). The mean annual temperature is 2–8 °C (Shi et al., 2018), and the altitude is more

than 1000 m above sea level. The main food crops grown are potato, wheat, and other minor food crops. Potato is sown mainly in the middle to late April, and harvested around October in the NSCZ. Potato grow in six stages: the germination stage (20–30 d), the seedling stage (15–20 d), the tuber-initiation stage (30 d), the tuber-bulking stage (15–25 d), the starch accumulation stage (20–30 d), and the mature stage (15–25 d)) (Hu et al., 2014). For the convenience of study, and based on the requirements of potato water consumption, we divided the potato growing period (GP) into: (1) the seedling stage (SS), including the germination stage, the seedling stage, and the tuber-initiation stage that last from April to June, (2) the tuber-growth stage (TS), which includes the tuber-bulking stage and the starch accumulation stage that occur during July and August, and (3) the mature stage (MS), lasting from September to the October harvest.

The monthly meteorological dataset used in this study was provided by the National Meteorological Information Center (http://data.cma.cn/). There are 43 meteorological stations in the NSCZ. Of these stations, most were established in the 1950s. The meteorological data for this study includes complete precipitation and temperature data from January 1960 to December 2016. The monthly SPEI was calculated according to the method of VicenteSerrano et al. (2010) using the station location, monthly cumulative rainfall, and mean monthly temperature. The potato production data from 1982 to 2016 were derived from the China Rural Statistical Yearbook published by National Bureau of Statistics of China. Data for each growth period are the averages of the SPEIs for the corresponding months.

2.2. Methods

2.2.1. Empirical orthogonal function

Empirical orthogonal function (EOF) analysis was first used for meteorological research by Lorenz (1956), and it is a commonly used diagnostic tool in meteorology. EOF analysis can depict the main features of complex spatiotemporal variables. In this study, the dominant patterns and variables of SPEIs were identified using EOF analysis. The output of EOF analysis includes spatial patterns (EOFs), time series (principal components, PCs), and eigenvalues (Liu et al., 2018). The North criterion was used to test for differences in modes (i.e., at the 95% confidence level, overlap between two errors indicates that there is no significant difference between the tested modes) (North et al., 1982).

2.2.2. Trend analysis methods

The Mann–Kendall statistical test was used to inspect the change tendency and to monitor the mutation point of the time coefficient (PCs). A UF > 0 indicates that the sequence has an upward trend; conversely, a UF < 0 indicates a decreasing trend. When UF exceeds the value of $Z = \pm 1.96$, it indicates a significant increase or decrease at the 95% confidence level. The intersection of UF and UB indicates an abrupt change at the corresponding time (Duan et al., 2016). The Mann–Kendall test is a non-parametric statistical method, and the trend test for time series is not affected by outliers. It can achieve statistical significance, but it cannot obtain the slope of the sequence. Sen's slope may be used to calculate the median value of a sequence slope, and it is robust to the influences of noise; however, it cannot judge the significance of a sequence trend. Therefore, the Mann–Kendall test and Sen's slope were combined to detect the trends in time series data effectively (Gocic and Trajkovic, 2013).

2.2.3. Grey theory analysis

The grey theory proposed by Deng (1982) provides a theoretical basis for the analysis, modeling, prediction, and control of systems with small sample sizes and limited information (Tien, 2012). In this study, grey correlation analysis following the methods of Liu and Yu (2007) was used to analyze the degree relationship between potato yield per unit area and the SPEI, wherein the potato yield per unit area values of the seven provinces in the NSCZ were used as the parent sequence and the average SPEIs of the GP, SS, TS, and MS in the corresponding provinces were used as son sequences. In Grey relation analysis, independent variables are considered to be the influencing factors when correlations are > 0.7, and the important factors for the correlation degree range from 0.5 to 0.7 (Han et al., 2017).

To determine the effect of drought on potato production, this study define climatic yield (CY_{it}) at year t in the ith province as $CY_{it} = Y_{it} - EY_{it}$ where Y_{it} is observed data (i.e., the potato yield per unit area) at year t in the ith province and EY_{it} is the expected yield value at year t in the ith province. Values of EY_{it} are estimated using local 'loess' regression models fitted to observed data. We used the 'loess' function in the R software with standard arguments (span = 0.75, degree = 2) (Fig. A.4). The method is used in similar settings in (Ben-Ari et al., 2016; Cernay et al., 2015). Understanding of the impacts of climatic factors on potato production has been limited by the ambiguity of the physical mechanisms at play and by the limited availability of statistical data on the national scale. Therefore, in this study, GM (1, N) (i.e., the grey predication model) was used to simulate the relationship between potato climatic yield and drought (i.e., PC1, equivalent here to the total change in dryness/wetness conditions in the NSCZ), along with the method from Ren et al. (2013).

2.2.4. Continuous wavelet transform

The continuous wavelet transform (CWT) is a powerful tool for analyzing nonstationary time series. It can decompose a signal in time and frequency space and also analyze and identify changes of dominant, localized variations in power (Liu et al., 2018). In this study, the CWT was used to analyze the periodic features of PCs. The method followed that of Torrence and Compo (1998).

2.2.5. Hurst exponent

The Hurst (H) exponent, which was introduced by Hurst (1951) to analyze Nile River hydrological time series, is an effective statistical method for judging the properties of time series without processing. The results may be compared with the theoretical value for an independent process of 0.5 using the estimated H. If $H = 0.5$, it indicates an independent process or a short-term independent process. $H > 0.5$ indicates that the process is a persistent process (i.e., the process has a significantly positive, non-accumulative autocovariance coefficient at all lag periods). $H < 0.5$ indicates that the process is an impermanent process (i.e., the process has a significant negative, non-accumulative autocovariance coefficient at all lag periods) (Barunik and Kristoufek, 2010).

2.2.6. Data analysis

In this study, EOF analysis, CWT, H exponent, Mann–Kendall statistical test, and Grey system analyses were completed in Matlab R2014a. The R package "trend" (https://cran.r-project.org/web/packages/trend/vignettes/trend.pdf) was used to implement the Mann–Kendall test and derive Sen's slope. ArcGIS 10.2 was used for kriging interpolation.

3. Results

3.1. NSCZ dryness/wetness conditions

Using the North criterion (Fig. A.1), the first two EOFs were chosen to explain the spatial pattern of dryness/wetness conditions for the GP, SS, TS, and MS. The cumulative contribution of the first two EOFs to the total variance was > 50%. In particular, EOF1 exceeded 30%. This indicates that a small number of spatial structures can be used to explain the complex characteristics of change in dryness/wetness conditions in the NSCZ.

The distribution of all EOF1 patterns revealed that the loading weights were positive, indicating that the dryness/wetness conditions were strongly coherent spatially (Fig. 2a–d). However, EOF2 revealed

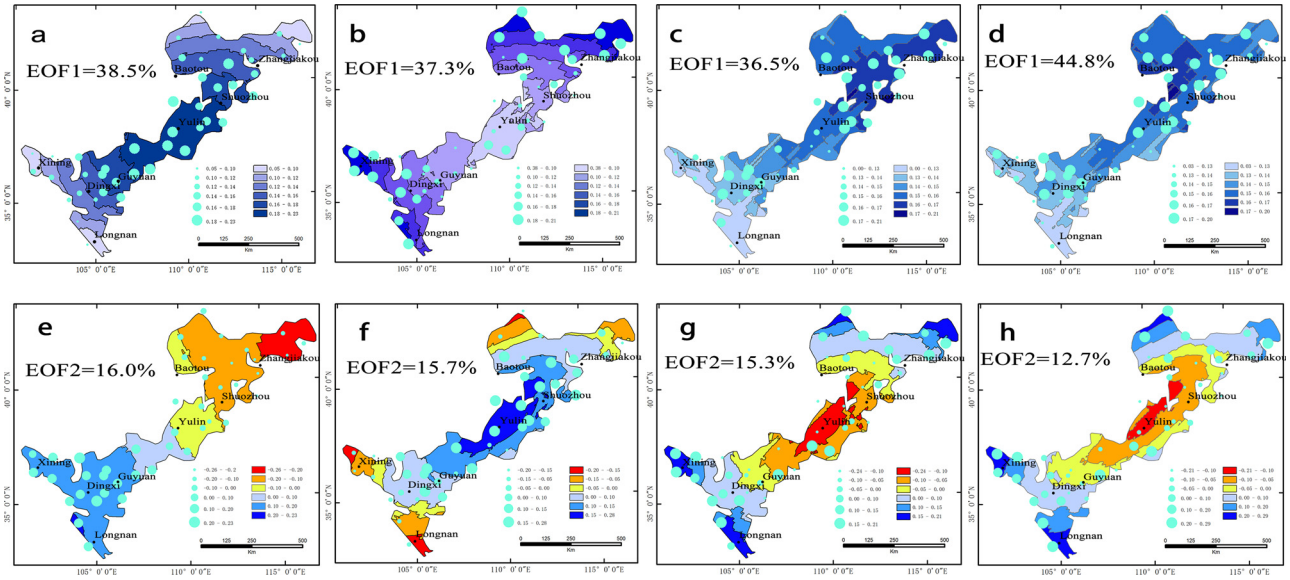

Fig. 2. Spatial patterns of the first two EOF modes of SPEI of the GP, SS, TS and MS. The first EOF mode of the GP (a), SS (b), TS (c), and (MS); the second EOF mode of the GP (e), SS (f), TS (g), and MS (h).

differences in the spatial distribution of the loading weights. EOF2 of the GP indicated a north–south difference in dryness/wetness conditions, in which positive loadings were concentrated mainly in the southern area and negative loadings were concentrated in the northern area (Fig. 2e). EOF2 of the SS, TS, and MS exhibited clear spatial differences among the central area around Yulin (the western part of the Loess Plateau), the northern area (the southwestern part of the Mongolian Plateau), and the southern area (the northeastern part of the Tibetan Plateau) (Fig. 2f–h).

The statistical results of the Mann–Kendall test of the corresponding PCs are shown in Fig. 3. PC1 of the GP revealed that the UF fluctuated about the zero line in the 1960s, but since 1970, the UF has been below the zero line (Fig. 3a). This indicated that the NSCZ continued to dry in the GP after 1970. However, the fact that UF always fluctuated near the zero line indicates that the SS was in an unstable state of alternating wet and dry conditions (Fig. 3b). For the TS and MS, although the spatial loading patterns exhibit similar characteristics, the polarity of the PC is in the opposite direction. As shown in Fig. 3c, the UF of the TS has remained positive since the 1970s. However, the UF of the MS became negative in 1968, has been fluctuating around −1.96 since 1974, but showed significant abrupt changes in 2010 (Fig. 3d). This indicates that the NSCZ has been relatively wet in the TS since the 1970s but that it has become significantly drier in the MS. For PC2 of the GP, SS, TS, and MS (Fig. 3e–h), the UF > 0 of the GP indicates that the southern area in the NSCZ was wetter than the northern area (Fig. 3e). PC2 is similar to PC1 in the SS, also indicating that spatial differences changed in an unstable, alternating manner (Fig. 3f). Fig. 3g shows that the UF of the TS became negative after 1975, and it has been lower than −1.96 since 1995. Conversely, the UF of the MS has remained positive since 1965 (Fig. 3h). This indicates that the western part of the Loess Plateau is relatively wet relative compared to the southwestern part of the Mongolian Plateau and the northeastern part of the Tibetan Plateau in the

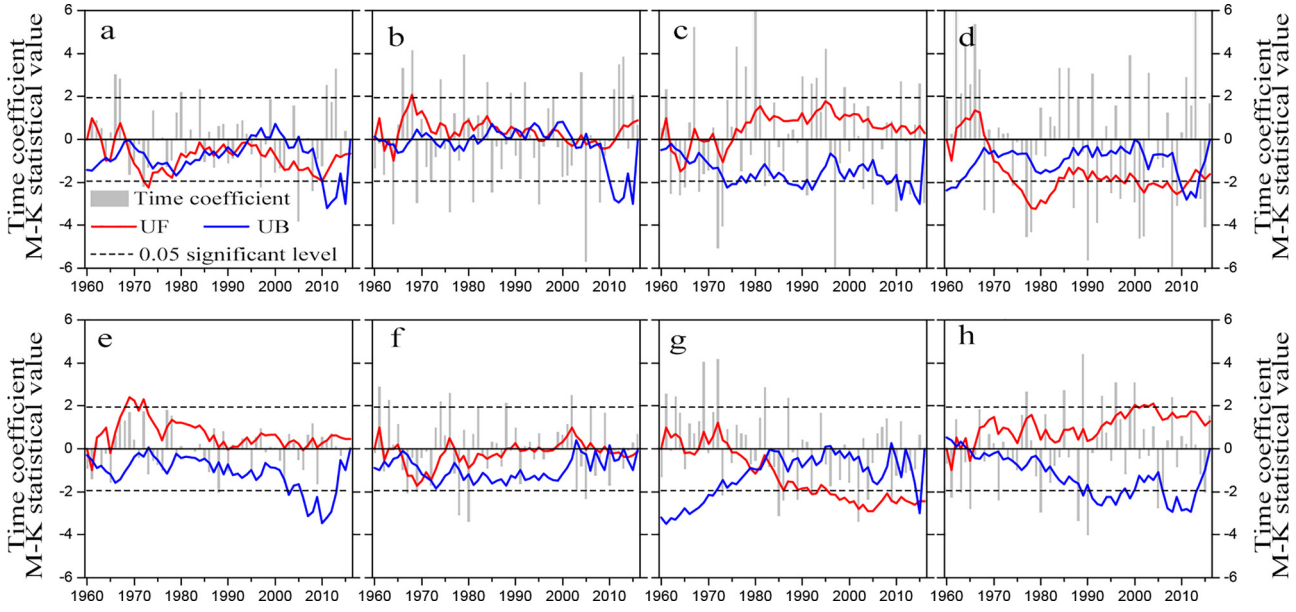

Fig. 3. Mann-Kendall statistical test of the corresponding time series principal components (PCs). PC1 of the GP (a), SS (b), TS (c), and MS (d); PC2 of the GP (e), SS (f), TS (g), and MS (h).

Table 1
Gray correlation degrees between potato yield per unit area and SPEIs of the GP, SS, TS and MS.

	GP	SS	TS	MS
Qinghai	0.9780	0.9840	0.6600	0.8034
Gansu	0.6473	0.8051	0.6264	0.8544
Ningxia	0.7977	0.7671	0.6001	0.9201
Shanxi	0.9760	0.9888	0.7147	0.9937
Shaanxi	0.8354	0.6611	0.8408	0.8668
Inner Mongolia	0.6551	0.9247	0.8501	0.9395
Hebei	0.6299	0.9256	0.9226	0.9521

TS. However, the western part of the Loess Plateau becomes relatively dry during the MS.

3.2. Potato production and drought

The results of the grey relation analysis revealed that all of the correlation degrees for the GP, SS, TS, and MS of all provinces in the NSCZ were > 0.6 (Table 1). Therefore, the changes in dryness/wetness conditions in the GP, SS, TS, and MS had important impacts on potato yield per area in the NSCZ.

The average climatic yield of potato was used as the dependent variable and PC1 of the SS, TS, and MS were used as the independent variables to establish the GM(1, N) model:

$$PN = (a, b1, b2, b3)^T = (-0.061, 25.015, 12.867, -6.875)^T,$$

where $a = -0.061$ represents the system development parameter, bi represents the driving parameter, and b1, b2, and b3 represent the affecting polarity and the extent of effect of dryness/wetness conditions of the SS, TS, and MS on the potato yield per unit area.

The results revealed that $|b1| > |b2| > |b3|$, i.e., that the dryness/wetness conditions of the SS had the greatest impact on the potato yield per unit area, followed by those of the TS and MS. The results also showed that b1 and b2 were positive, while b3 was negative. This indicates that wetness during the MS had a negative impact on potato production but that wetness during the SS and TS had a positive effect. The results of climatic fluctuant yield showed that the fluctuations of potato climatic yields were more consistent among the seven provinces before 2000 but less consistent after 2000 (Fig. A.5a). Similarly, the GM (1, N) model can better simulate the relationship between climatic yield and PC1 before 2000; however, the difference between actual climate production and simulated production is large after 2000 (Fig. A.5b).

3.3. Periodic features and drought trends

3.3.1. Periodic features

The continuous wavelet power spectra for the PC1 time series for the GP, SS, TS, and MS are shown in Fig. 4. The significant wavelet power spectra of the GP (Fig. 4a) were the 4–5 year and 1–5 year bands, which occurred during 1975–1985 and 1998–2005, respectively. Meanwhile, there was one nonsignificant band of 3–8 years in 1964–1974. The wavelet power spectra for the SS were broadly distributed, with 1–2 year bands during 1968–1970 and 1978–1980, 1–3 year bands during 2002–2005, and 5–6 year bands during 1978–1988 and 1990–2000; nonsignificant 7–8 year bands were also found during 1968–1972 (Fig. 4b). The wavelet power spectra of the TS exhibited 3–5 year, 1 year, 3–4 year, and 5–8 year bands during 1968–1982, 1975–1980, 1993–1998, and 1990–2000, respectively; there were also two nonsignificant bands of 14–16 years (during 1972–1990) and 2–3 years (during 2010–2014) (Fig. 4c). For the MS, power was relatively slightly distributed, and the only significant bands were 1–3 year bands and 4–5 year bands that occurred during 1988–1992 and 2000–2005, respectively. Additionally, there were nonsignificant 2–3 year, 7–8 year, and 18–30 year bands during 2010–2016, 2005–2016, and 1960–1994, respectively (Fig. 4d). Lastly, the wavelet power and wavelet spectra of PC2 exhibited spatial differences in SPEI, which are provided as supplemental material (Fig. A.2).

3.3.2. Future drought trends

The Mann–Kendall test and Sen's slope were used to calculate the significance and the slope of the PC1 time series, respectively. H exponent was used to predict the persistence of changes in dryness/wetness conditions. The significance, slope, and H exponent of PC1 for the GP, SS, TS, and MS are shown in Table 2. The Sen's slopes of the GP and MS were −0.00685 (Z = 0.640, p = 0.522) and −0.04606 (Z = −1.604, p = 0.109), and the H exponents were 0.610 and 0.644, respectively. Therefore, the NSCZ becomes drier in the GP and MS, and the drought trend predicted for the future is consistent with the current state. The Sen's slopes of the SS and TS were 0.01788 (Z = 0.888, p = 0.375) and 0.00565 (Z = 0.282, p = 0.778), and the H exponents were 0.515 and 0.675, respectively. Therefore, the NSCZ will become wetter in the SS and TS, and this predicted trend is also consistent with the current state. However, the persistence of changes during the SS was weak, with Grade I persistent strength. This further indicates the instability of the trend of dryness/wetness conditions in the SS. Although the persistence strength of the TS was stronger, Grade III, it exhibited the smallest slope (Table 3).

The points in Fig. 5 reflect the spatial distribution of the Sen's slopes and H exponents of the SPEIs at the 43 stations in the NSCZ. The results revealed that for the GP, SS, TS, and MS, 69.8%, 18.6%, 58.1%, and 81.4% of the stations exhibited a Sen's slope < 0, respectively. Among the 43 stations, 95.3% (GP), 73.4% (SS), 88.4% (TS), and 88.4% (MS) of the stations exhibited an H exponent > 0.5. Therefore, declining (i.e., drying) trends of SPEI were found at most stations for the GP and MS. Moreover, the SPEI of 30.2% of the stations exhibited a significant decrease during the MS. Although the SPEIs of most stations were increased in the SS, they were not significant (p < 0.05). In the TS, the SPEI of the stations north of Yulin is increased but that of the stations to the south is decreased. The persistence of change from H exponent indicated that future trends at most of the stations will be consistent with the current status. To explore the trend of future changes of dryness/wetness conditions further, we spatially overlaid the results of the Sen's slopes and H exponents (Fig. 5e–h). The results indicated that the MS as a whole will become drier in the future. However, the spatial continuities of the GP, TS and SS were poor.

4. Discussion

The NSCZ is an arid and semiarid region. Climate change has intensified the frequency and severity of droughts, leading to water shortages, crop failures, and ecological deterioration (Liu et al., 2018). Potato is the most important crop in the NSCZ (Hu et al., 2014). Therefore, this study analyzed the relationship between potato production and drought in the NSCZ, the characteristics of spatiotemporal changes of drought and future trends based on the SPEI drought index.

4.1. Using grey theory to explore the relationship between potato production and drought

Potato is a relatively shallow-rooted crop compared with other leguminous and field crops. Potato is therefore more susceptible to drought stress in arid and semiarid regions with high transpiration demand and low soil water holding capacities (Qin et al., 2012). Similarly, our results also revealed that the changes in dryness/wetness conditions in the four periods (i.e., GP, SS, TS, and MS) across the seven provinces in the NSCZ all have important impacts on potato production (Section 3.2).

The GM (1, N) model results indicated that drought has a relatively small positive impact on potato production during the MS but a

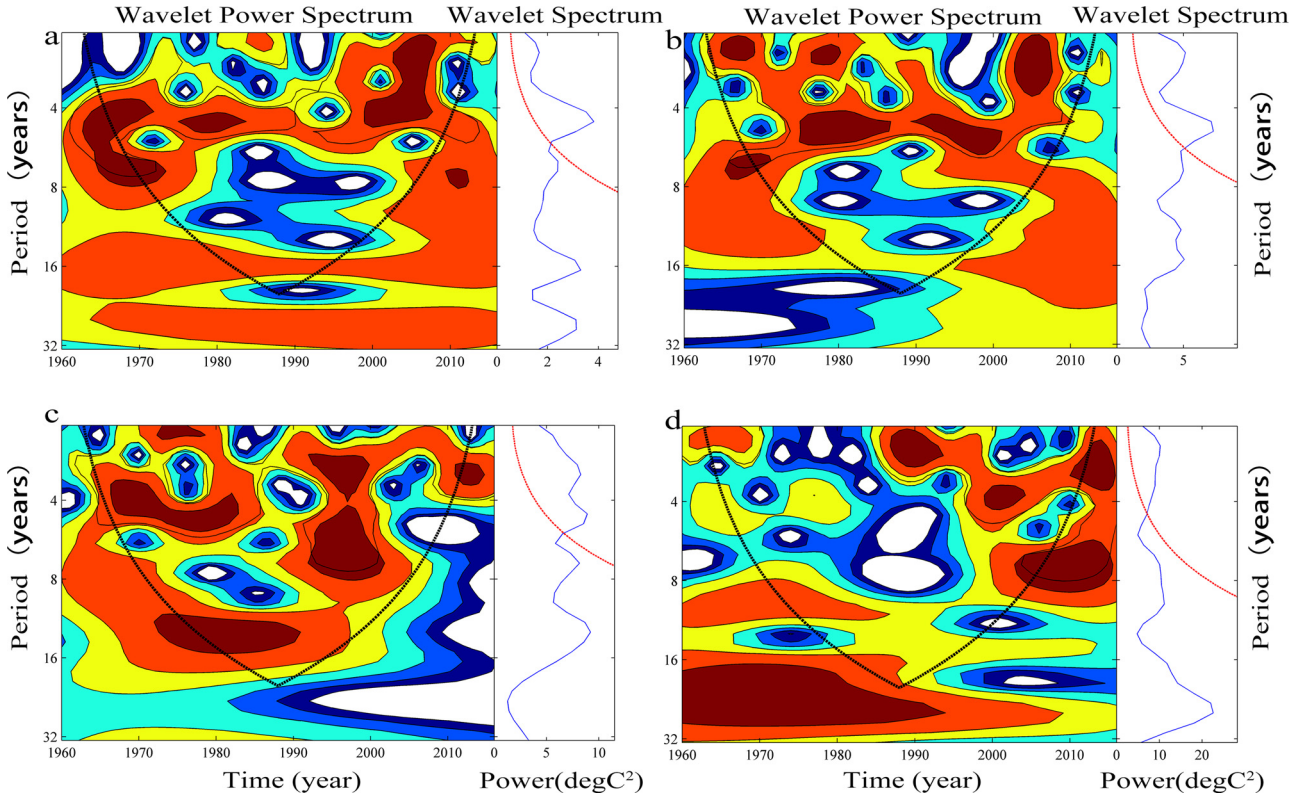

Fig. 4. Continuous wavelet power spectrum and wavelet spectrum of PC1 of the GP (a), SS (b), TS (c), and MS (d) from 1960 to 2016.
Note: The thick black contours designates the 95% confidence level against red noise and the black line is cone of influence (COI) beyond which the picture may be distorted by the effect of zero padding.

Table 2
Results of Mann-Kendall test, Sen's slope, and the Hurst exponent.

Time	Z	Sen's slope	p	H
GP	−0.640	−0.00685	0.522	0.610
SS	0.888	0.01788	0.375	0.515
TS	0.282	0.00565	0.778	0.675
MS	−1.604	−0.04606	0.109	0.644

relatively large negative effect during the SS and TS (Section 3.2). The work of Shock (2010) indicated that daily water needs increase rapidly from emergence until about two weeks after row closure. From this time onward, the daily water requirements of the potato plants remain nearly constant until the vines begin to mature, after which water requirements decline rapidly. During the early growth stage, drought stress will close the stomata, and prolonged drought stress will stop the growth and development of the tuber, leading to a reduction in yield (Qin et al., 2012). Therefore, water availability during the SS and TS has important impacts on potato production. The NSCZ experiences higher rainfall and increased temperatures during the same period, July–September (Fig. A.6). This results in relatively small impacts of changes in dryness/wetness conditions in the TS. However, excessive rainfall can cause the specific gravity of potato tubers to decrease, tuber rot, and intolerance storage when the potato matures (Qin et al., 2012). Therefore, excessive water supply can negatively affect potato yield in the MS.

4.2. Spatiotemporal changes in dryness/wetness conditions

Based on the EOF analyses, the first two EOFs, which together account for > 50% of the total variance, can be used to explain the spatial patterns of dryness/wetness conditions for the GP, SS, TS, and MS. All EOF1s were spatially distributed with positive loadings and contributed > 30% of the total variance, revealing the total trend of changes in dryness/wetness conditions in the NSCZ. The explanation of the variance by EOF1 is likely because the NSCZ is located in marginal regions of the Asian monsoon and is mainly affected by the Asian monsoon (Li et al., 2012). Therefore, the EOF1 pattern reflects the circumstance that the dryness/wetness conditions in the NSCZ are mainly controlled by the same large-scale weather system. Time series

Table 3
Classification of Hurst exponent and SPEI (Tong et al., 2018; Wu et al., 2017).

Grade	Hurst exponent			SPEI	
	Positive correlation	Negative correlation	Strength	Value	Strength
I	0.50 < H ≤ 0.55	0.45 < H ≤ 0.50	Weak	1 < SPEI	Severe wet
II	0.55 < H ≤ 0.65	0.35 < H ≤ 0.45	Weaker	0.5 < SPEI ≤ 1	Moderate wet
III	0.65 < H ≤ 0.75	0.25 < H ≤ 0.35	Stronger	0 < SPEI ≤ 0.5	Near normal
IV	0.75 < H ≤ 0.85	0.15 < H ≤ 0.25	Strong	−0.5 < SPEI ≤ 0	Light drought
V	0.85 < H ≤ 1.00	0.00 < H ≤ 0.15	Very strong	−1 < SPEI ≤ −0.5	Moderate drought
				SPEI ≤ −1	Severe drought

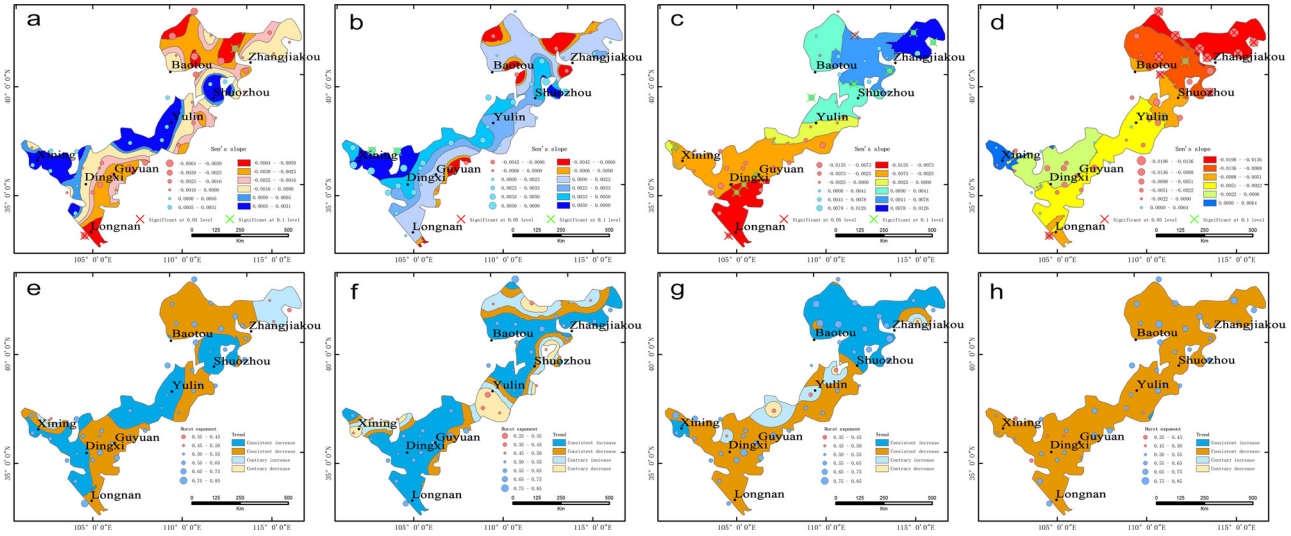

Fig. 5. Spatial distribution and interpolated maps of Sen's slope and H-values of the SPEI time series at 43 stations from 1960 to 2016. Interpolated maps of Sen's slopes of the GP (a), SS (b), TS (c), and MS (d). Spatial overlay maps of Sen's slope and H exponent of the GP (e), SS (f), TS (g), and MS (h).

analysis revealed that the NSCZ tended to become drier in the GP since the 1970s. The results presented here are consistent with those of Dai et al. (2004) and Zou et al. (2005) and support their notion that there has been increased risk of drought since the late 1970s as global warming has produced both higher temperatures and increased drying. However, the dryness/wetness conditions of the SS showed an unstable alternating state, the TS slowly became wetter from the 1970s, and the MS began to experience significant drought from the 1970s. Ren et al. (2004) demonstrated that the spring rainfall in the eastern part of northwest China is affected by the Asian monsoon and the Tibetan Plateau and that the rainfall variability is relatively large. This variability led to a significant, unstable change in dryness/wetness conditions in the SS. The dryness/wetness conditions in the NSCZ are affected mainly by the Asian monsoon, which leads to more rainfall in summer (Shi et al., 2007). However, the work of Wang (2001) revealed that the Asian summer monsoon has weakened since the 1960s, which may further aggravate the impacts of drought in the MS. These results are also consistent with the findings of Yao et al. (2013).

EOF2, which contributed > 10% of the total variance, indicated spatial differences in dryness/wetness conditions. Wang et al. (2015) indicated that drought conditions differ between northern and southern China due to the effects of atmospheric circulation and plateau topography. Similarly, drought during the GP also exhibits a difference between the north and south regions of the NSCZ. Meanwhile, the SS, TS, and MS exhibited spatial differences in dryness/wetness conditions between the western part of the Loess Plateau and the southwestern part of the Mongolian Plateau and northeastern part of the Tibetan Plateau. This pattern may be caused by the low pressure system over India, the Bay of Bengal, and the North Arabian Sea, which is highly correlated with the increases of water vapor flux during the Asian summer monsoon, and the western Pacific subtropical high could promote water vapor transportation, which causes dryness/wetness conditions in the upper reaches of the Yellow River to differ from those of other regions in the marginal areas of the Asian monsoon (Li et al., 2012). This study focused on the total changes in dryness/wetness conditions in the NSCZ, so no further analysis of PC2 was conducted.

4.3. Periodic features and trends of drought changes

Periodic features and trends are two important characteristics of drought time series. Because of the location of the NSCZ, the periodic alternation of relatively dry and wet years is caused by the thermal and dynamic effects of the plateau terrain and the interannual variation in the prevailing circulation (Song, 2005). In this study, dryness/wetness conditions in the GP, SS, TS, and MS were analyzed by CWT. The results revealed that changes in dryness/wetness conditions have significant multi-timescale periodic oscillation features in the GP, SS, TS, and MS. Although many studies have examined periodic changes in dryness/wetness conditions, the specific reasons for the oscillatory behavior on multi-year scales have not yet been understood fully (Liu et al., 2018; Tong et al., 2018; Wen et al., 2017). Further research is needed.

The work of Tong et al. (2018) demonstrated that the H exponent exhibits an accuracy of 91.7% for predicting drought trends. Therefore, we combined the Mann–Kendall test, Sen's slope, and H exponent to predict the trend of drought in the NSCZ. The results indicated that the NSCZ will have a tendency to become wetter in the SS and TS. However, the Sen's slope of the TS was the smallest, and the H exponent of the SS was the smallest, indicating weak trend persistence. There was a tendency toward drought in the MS, which also exhibited the largest Sen's slope and H exponent. The trend analysis of the SPEIs for 43 stations suggested that the NSCZ, as a whole, will become drier in the future during the MS (Section 3.3.2).

4.4. Limitations and implications

In this study, we conducted a systematic analysis of potato production with respect to changes in dryness/wetness throughout the growing season. However, before considering the implications of this work, limitations of the study should be noted. First, the works of Ren et al. (2013) and Ren (2018) showed that the GM (1, N) model had good prediction power. However, because PC1, which explained 30% of the total variance, was used as an independent variable and because the dependent variable used in this study was potato yield derived from national statistical data, the prediction function of the model performed poorly in this study (Fig. A.5b). Therefore, further research that relies on field measurement data is needed. The second limitation of the study arose from our use of potato production data extending only from 1982 to 2016 due to limitations of national statistical data. Finally, although the H exponent has a high degree of accuracy in predicting drought trends, H exponent cannot predict how long the anticipated drought will continue into the future.

Bearing in mind the limitations of this study, our results indicate that because potato is a sensitive crop with respect to water stress, drought has a greater impact on potato production in the NSCZ. By implementing crop management measures, including feasible late sowing by staggering the water critical period of potato growth, making

full use of rainfall by improving cultivation and management practices, and cultivating drought-resistant potato cultivars, potato production in the NSCZ may be promoted.

5. Conclusions

In this study, we examined the relationship between drought and potato production and analyzed the spatial and temporal characteristics, periodicity, and subsequent trends of drought over the NSCZ during the period of 1960–2016. First, based on the SPEI drought index of the potato growing period (GP, SS, TS, and MS), EOF analysis identified two significant EOFs and corresponding PCs. EOF1 was the overall drought pattern of the NSCZ as a whole, and EOF2 was the pattern of drought spatial difference. Then, the relationship between drought (i.e., PC1) and potato production in the NSCZ was explored using grey theory. The results indicated that drought in SS and TS had relatively large negative effects on potato production, whereas drought in MS had a relatively small positive effect. Finally, the periodic oscillation features of drought were analyzed by CWT. The results revealed that the changes in dryness/wetness conditions include significant multi-timescale periodic oscillation features. In addition, the Mann–Kendall statistical test, H exponent, Mann–Kendall test, and Sen's slope were used to explore the spatiotemporal tendencies of drought. The results showed that the NSCZ continued to dry after the 1970s in the GP and MS but that it became relatively more wet in the TS. However, the SS remained in an unstable state of alternating wet and dry conditions. Additionally, the H exponent showed that the future drought trend is generally consistent with the current state for GP, SS, TS, and MS. Moreover, it is worth noting that the NSCZ as a whole will become drier in the MS. Drought has a greater impact on the ecological and agricultural production of the monsoon marginal zone. This study provides a theoretical basis for the study of drought and the breeding and management of potato in the monsoon-affected NSCZ.

Acknowledgment

This work was supported by Basic Work of Science and Technology Special Project: Survey on Land Utilization and Agricultural Nonpoint Source Pollution Around South-To-North Water Diversion (Mid-Line) (2015FY110400-3).

Appendix A. Supplementary data

Supplementary material related to this article can be found, in the online version, at doi:https://doi.org/10.1016/j.agrformet.2018.10.019.

References

Banik, P., Zeng, W.P., Tai, H., Bizimungu, B., Tanino, K., 2016. Effects of drought acclimation on drought stress resistance in potato (Solanum tuberosum L.) genotypes. Environ. Exp. Bot. 126, 76–89.
Barunik, J., Kristoufek, L., 2010. On Hurst exponent estimation under heavy-tailed distributions. Phys. A Stat. Mech. Appl. 389, 3844–3855.
Beguería, S., Vicente-Serrano, S.M., Angulo-Martínez, M., 2010. A multiscalar global drought dataset: the SPEI base: a new gridded product for the analysis of drought variability and impacts. Bull. Am. Meteorol. Soc. 91, 1351–1356.
Ben-Ari, T., Adrian, J., Klein, T., Calanca, P., Van der Velde, M., Makowski, D., 2016. Identifying indicators for extreme wheat and maize yield losses. Agric. For. Meteorol. 220, 130–140.
Cernay, C., Ben-Ari, T., Pelzer, E., Meynard, J.-M., Makowski, D., 2015. Estimating variability in grain legume yields across Europe and the Americas. Sci. Rep. 5.
Dai, A., 2011. Erratum: drought under global warming: a review. Wiley Interdiscip. Rev. Clim. Change 2, 45–65.
Dai, A., Trenberth, K.E.E., Qian, T., 2004. A global dataset of palmer drought severity index for 1870–2002: relationship with soil moisture and effects of surface warming. J. Hydrometeorol. 5, 1117–1130.
Deng, J.L., 1982. Control problems of grey systems. Syst. Control Lett. 1, 288–294.
Duan, X.W., Gu, Z.J., Li, Y.G., Xu, H.J., 2016. The spatiotemporal patterns of rainfall erosivity in Yunnan Province, southwest China: an analysis of empirical orthogonal functions. Glob. Planet. Change 144, 82–93.
Evers, D., Lefevre, I., Legay, S., Lamoureux, D., Hausman, J.F., Rosales, R.O.G., et al., 2010. Identification of drought-responsive compounds in potato through a combined transcriptomic and targeted metabolite approach. J. Exp. Bot. 61, 2327–2343.
Gocic, M., Trajkovic, S., 2013. Analysis of changes in meteorological variables using Mann-Kendall and Sen's slope estimator statistical tests in Serbia. Glob. Planet. Change 100, 172–182.
Han, X., Liu, Y., Gao, H., Ma, J., Mao, X., Wang, Y., et al., 2017. Forecasting PM2.5 induced male lung cancer morbidity in China using satellite retrieved PM2.5 and spatial analysis. Sci. Total Environ. 607–608, 1009–1017.
Haverkort, A.J., Verhagen, A., 2008. Climate change and its repercussions for the potato supply chain. Potato Res. 51, 223–237.
Hijmans, R.J., 2003. The effect of climate change on global potato production. Am. J. Potato Res. 80, 271–279.
Hu, Q., Pan, F., Pan, X., Zhang, D., Yang, N., Pan, Z., et al., 2014. Effects of a ridge-furrow micro-field rainwater-harvesting system on potato yield in a semi-arid region. Field Crops Res. 166, 92–101.
Hurst, H.E., 1951. Long term storage capacity of reservoirs. Trans. Am. Soc. Civil Eng. 116, 776–808.
Jansky, S.H., Jin, L.P., Xie, K.Y., Xie, C.H., Spooner, D.M., 2009. Potato production and breeding in China. Potato Res. 52, 57.
Li, Y., Na, Wang, Chen, H., Li, Z., Zhou, X., Zhang, C., 2012. Tracking millennial-scale climate change by analysis of the modern summer precipitation in the marginal regions of the Asian monsoon. J. Asian Earth Sci. 58, 78–87.
Liu, G., Yu, J., 2007. Gray correlation analysis and prediction models of living refuse generation in Shanghai city. Waste Manag. 27, 345–351.
Liu, Z., Zhou, P., Zhang, F., Liu, X., Chen, G., 2013. Spatiotemporal characteristics of dryness/wetness conditions across Qinghai Province, Northwest China. Agric. For. Meteorol. 182–183, 101–108.
Liu, Z.Y., Zhang, X., Fang, R.H., 2018. Multi-scale linkages of winter drought variability to ENSO and the Arctic Oscillation: a case study in Shaanxi, North China. Atmos. Res. 200, 117–125.
Lobell, D.B., Field, C.B., 2007. Global scale climate - crop yield relationships and the impacts of recent warming. Environ. Res. Lett. 2, 7.
Lorenz, E.N., 1956. Empirical Orthogonal Functions and Statistical Weather Prediction. Scientific Report No. 1. 409. MIT, Cambridge, MA, pp. 1–49.
Lu, W., Jia, G., 2013. Fluctuation of farming-pastoral ecotone in association with changing East Asia monsoon climate. Clim. Change 119, 747–760.
Monneveux, P., Ramirez, D.A., Pino, M.T., 2013. Drought tolerance in potato (S. tuberosum L.) Can we learn from drought tolerance research in cereals? Plant Sci. 205, 76–86.
North, G.R., Bell, T.L., Cahalan, R.F., Moeng, F.J., 1982. Sampling errors in the estimation of empirical orthogonal functions. Mon. Weather Rev. 110, 699–706.
Obidiegwu, J.E., Bryan, G.J., Jones, H.G., Prashar, A., 2015. Coping with drought: stress and adaptive responses in potato and perspectives for improvement. Front. Plant Sci. 6.
Policy Plan, 2009. Chinese Potato Superior Regional Layout Planning (2008–2015). Agriculture Engineering Technology (Agricultural Product Processing Industry), pp. 4–7 in Chinese.
Qin, S., Li, L., Wang, D., Zhang, J., Pu, Y., 2012. Effects of limited supplemental irrigation with catchment rainfall on rain-fed potato in semi-arid areas on the Western Loess Plateau, China. Am. J. Potato Res. 90, 33–42.
Ren, H., Zhang, P., Gao, L., 2004. Characteristics of precipitation and water vapor transport during springtime in the eastern northwest China. Acta Meteorol. Sin. 62, 365–374.
Ren, J., Gao, S., Tan, S., Dong, L., 2013. Prediction of the yield of biohydrogen under scanty data conditions based on GM(1, N). Int. J. Hydrogen Energy 38, 13198–13203.
Ren, J.Z., 2018. GM(1,N) method for the prediction of anaerobic digestion system and sensitivity analysis of influential factors. Bioresour. Technol. 247, 1258–1261.
Shi, W., Liu, Y., Shi, X., 2018. Contributions of climate change to the boundary shifts in the farming-pastoral ecotone in northern China since 1970. Agric. Syst. 161, 16–27.
Shi, Y., Shen, Y., Kang, E., Li, D., Ding, Y., Zhang, G., et al., 2007. Recent and future climate change in Northwest China. Clim. Change 80, 379–393.
Shock, C., 2010. Water requirements and irrigation. In: In: Bohl, W.H., Johnson, S.B. (Eds.), Commercial Potato Production in North America (The Potato Association of America Handbook), Supplement vol. 57 The Potato Association of America pp. 54.
Song, L., 2005. Study on Arid Climate Change in the Northwest of China and its Response to Global Warming. NanJing University of Information Science & Technology.
Tao, F., Yokozawa, M., Xu, Y., Hayashi, Y., Zhang, Z., 2006. Climate changes and trends in phenology and yields of field crops in China, 1981–2000. Agric. For. Meteorol. 138, 82–92.
Tian, Y., Su, D., Li, F., Li, X., 2003. Effect of rainwater harvesting with ridge and furrow on yield of potato in semiarid areas. Field Crops Res. 84, 385–391.
Tien, T.-L., 2012. A research on the grey prediction model GM(1,n). Appl. Math. Comput. 218, 4903–4916.
Tong, S., Lai, Q., Zhang, J., Bao, Y., Lusi, A., Ma, Q., et al., 2018. Spatiotemporal drought variability on the Mongolian Plateau from 1980-2014 based on the SPEI-PM, intensity analysis and Hurst exponent. Sci. Total Environ. 615, 1557–1565.
Torrence, C., Compo, G.P., 1998. A practical guide to wavelet analysis. Bull. Am. Meteorol. Soc. 79, 61–78.
VicenteSerrano, S.M., Beguería, S., LópezMoreno, J.I., 2010. A multiscalar drought index sensitive to global warming: the standardized precipitation evapotranspiration index. J. Clim. 23, 1696–1718.
Walther, G.-R., Post, E., Convey, P., Menzel, A., Parmesan, C., Beebee, T.J.C., et al., 2002. Ecological responses to recent climate change. Nature 416, 389.
Wang, C.-C., Wang, X.-Y., Wang, K.-X., Hu, J.-J., Tang, M.-X., He, W., et al., 2018. Manipulating aeroponically grown potatoes with gibberellins and calcium nitrate.

Am. J. Potato Res.
Wang, H., 2001. The weakening of the Asian monsoon circulation after the end of 1970's. Adv. Atmos. Sci. 18, 376–386.
Wang, Z., Jiang, J., Liao, Y., Deng, L., 2015. Risk assessment of maize drought hazard in the middle region of farming-pastoral ecotone in Northern China. Nat. Hazards 76, 1515–1534.
Wen, X.H., Wu, X.Q., Gao, M., 2017. Spatiotemporal variability of temperature and precipitation in Gansu Province (Northwest China) during 1951-2015. Atmos. Res. 197, 132–149.
Wu, L., Wang, S., Bai, X., Luo, W., Tian, Y., Zeng, C., et al., 2017. Quantitative assessment of the impacts of climate change and human activities on runoff change in a typical karst watershed, SW China. Sci. Total Environ. 601, 1449–1465.
Yactayo, W., Ramirez, D.A., Gutierrez, R., Mares, V., Posadas, A., Quiroz, R., 2013. Effect of partial root-zone drying irrigation timing on potato tuber yield and water use efficiency. Agric. Water Manag. 123, 65–70.
Yao, N., Li, Y., Lei, T., Peng, L., 2018. Drought evolution, severity and trends in mainland China over 1961–2013. Sci. Total Environ. 616–617, 73–89.
Yao, Y., Wang, R., Yang, J., Yue, P., Lu, D., Xiao, G., et al., 2013. Changes in terrestrial surface dry and wet conditions on the Loess Plateau (China) during the last half century. J. Arid Land 5, 15–24.
Yuan, L., Wang, E.L., Yang, X.G., Jing, W., 2010. Contributions of climatic and crop varietal changes to crop production in the North China Plain, since 1980s. Glob. Change Biol. 16, 2287–2299.
Zhao, H., Wang, R.-Y., Ma, B.-L., Xiong, Y.-C., Qiang, S.-C., Wang, C.-L., et al., 2014. Ridge-furrow with full plastic film mulching improves water use efficiency and tuber yields of potato in a semiarid rainfed ecosystem. Field Crops Res. 161, 137–148.
Zhao, W., Hu, Z., Li, S., Guo, Q., Liu, Z., Zhang, L., 2017. Comparison of surface energy budgets and feedbacks to microclimate among different land use types in an agro-pastoral ecotone of northern China. Sci. Total Environ. 599–600, 891–898.
Zou, X., Zhai, P., Zhang, Q., 2005. Variations in droughts over China: 1951–2003. Geophys. Res. Lett. 32.